



**A CRYSTALLOGRAPHIC OPTIMIZATION STUDY IN
TA/TAN BI-LAYER SPUTTERING TO REDUCE
SEMICONDUCTOR MANUFACTURING QUEUE
TIME CONSTRAINT.**

ANUAR FADZIL BIN AHMAD

DOCTOR OF ENGINEERING

2022



Faculty of Manufacturing Engineering

A CRYSTALLOGRAPHIC OPTIMIZATION STUDY IN TA/TAN BI-LAYER SPUTTERING TO REDUCE SEMICONDUCTOR MANUFACTURING QUEUE TIME CONSTRAINT.

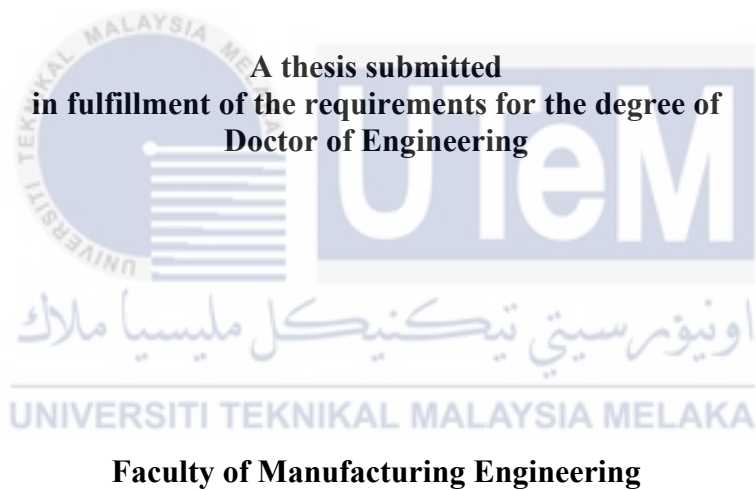
Anuar Fadzil Bin Ahmad

Doctor of Engineering

2022

**A CRYSTALLOGRAPHIC OPTIMIZATION STUDY IN TA/TAN BI-LAYER
SPUTTERING TO REDUCE SEMICONDUCTOR MANUFACTURING QUEUE
TIME CONSTRAINT.**

ANUAR FADZIL BIN AHMAD



UNIVERSITI TEKNIKAL MALAYSIA MELAKA

2022

DECLARATION

I declare that this thesis entitled “Manufacturing Constraint Mitigation through Improvement of Cu barrier seed Film Ageing Characteristics Using DOE Approaches” is the result of my own research except as cited in the references. The thesis has not been accepted for any degree and is not concurrently submitted in candidature of any other degree.



Signature : 

UNIVERSITI TEKNIKAL MALAYSIA MELAKA

Name: : Anuar Fadzil Bin Ahmad

Date : 5 February 2022

APPROVAL

I hereby declare that I have read this thesis and in my opinion, this thesis is sufficient in terms of scope and quality for the award of Doctor of Engineering.

Signature : 

Supervisor's Name: : MD NIZAM BIN ABD RAHMAD

Date : 5/2/2022



اونيورسيتي تيكنيكل مليسيا ملاك
UNIVERSITI TEKNIKAL MALAYSIA MELAKA

DEDICATIONS

All praise belongs to Allah.

To all Silterrans and the great company we are associated with and to my beloved family
for your support patience and understanding



ABSTRACT

The Physical Vapor Deposition (PVD) magnetron sputtering method is the most extensively used technique for depositing metallic thin film in the semiconductor wafer fabrication industry. The PVD equipment manufacturer has specified stringent control, in this case, a queue time restriction between the Copper (Cu) barrier seed layer and the following Cu electroplating layer deposition processes. This restriction is formed without providing detailed data or reasoning. This is applied as a condition to safeguard the interconnect quality and performance from functionality and reliability performance failures. Consequently, the queue time has imposed plenty of manufacturing challenges. In cases when the PVD and electroplating processes have to be stopped, the queue time cannot be exceeded and this creates constraints that lead to evasive steps that can create a capacity bottleneck that risks failure in the on-time delivery. The objective of this research is to investigate the film characteristics change in Cu electroplating film against queue time impact in order to verify the need to uphold queue time requirement recommended by the tool manufacturer. In pursuit of this, baseline film ageing characteristics that include sheet resistance and microstructure studies over an ageing period are planned out and compared to the peer studies. The comparisons prompted improvement in Ta bi-layer α -Ta crystal texture content which is shown to result in higher Cu (111) crystal texture and promoted sheet resistance (R_s) stability in the interconnect stack. In order to improve the metal film stability, a screening analysis of variance (ANOVA) experiment was conducted. A fractional factorial experiment was planned out to study the impact of TaN bias power, nitrogen flow rate, Cu bias power, and re-sputter layer on both the Cu barrier seed layer and the Cu electroplating stacked on Cu barrier seed layer. The impact study is primarily on film R_s ageing properties. A statistically significant parameter that influences the R_s stability for both layers is re-sputter treatment layer. Microstructural x-ray diffraction (XRD) analysis is done to understand the ageing mechanism. Next, selected screening experiment parameter settings, along with control, have been used in a wide range of queue time intervals between Cu barrier seed and Cu electroplating processes to understand the impact of the queue time on Cu Electroplating film R_s stability. The results show a stable R_s to an interval of 40 hours. It is also learnt that the cell with re-sputter done on TaN layer has stability up to almost four times compares to the standard manufacturing process cell. The application of TaN layer re-sputter has also shown a higher level of α -Ta ratio content with respect to β -Ta which in turn produces more, of the preferred Cu (111) grains. This research went a step further to have a prediction model to minimize R_s mean and non-uniformity changes during ageing by using the TaN re-sputter process in an RSM experiment. TaN re-sputter impact has again shown its dominance over other modeled parameters causing an insignificant model fit for mean R_s . Additionally, a prediction model is successfully generated for R_s non-uniformity at 48 hours ageing period.

KAJIAN PENGOPTIMUMAN KRISTALOGRAFI PADA LOGAM TA/TAN DWI-LAPISAN UNTUK MENGURANGKAN KEKANGAN MASA MENUNGGU DALAM PEMBUATAN SEMIKONDUKTOR

ABSTRAK

Kaedah pelapisan secara magnetron PVD adalah paling banyak digunakan untuk penyaduran filem logam nipis dalam pembuatan wafer semikonduktor. Pengeluar peralatan PVD telah menetapkan kawalan ketat dalam peruntukan sekatan waktu menunggu di antara proses pelapisan benih penghalang kuprum dan proses pelapisan elektrolisis kuprum tanpa memberikan data dan sebab. Ini dianggap perlu untuk melindungi kualiti dan prestasi lapisan logam daripada kegagalan fungsi dan ketahanan. Ini telah memberi cabaran dalam proses pembuatan. Apabila proses PVD dan elektrolisis perlu dihentikan, masa pemberhentian tidak boleh dianjali dan ini mewujudkan kekangan yang boleh mengakibatkan kegagalan penghantaran produk kepada pelanggan. Objektif penyelidikan ini adalah untuk menyelidik kesan tempoh menunggu bagi menentukan keperluan mematuhi kekangan tempoh menunggu. Untuk ini, penyelidikan sifat penuaan filem yang merangkumi perubahan rintangan logam nipis dan mikrostruktur logam sepanjang tempoh penuaan telah dianjurkan. Ia mengambil kira maklumat penyelidikan setara. Ini mendorong kepada peningkatan α -Ta dalam logam Ta dwi-lapisan dan tekstur kristal Cu(111) yang telah menggalakkan kestabilan rintangan logam. Bagi lebih meningkatkan kestabilan filem, kaedah ANOVA digunakan bagi mengkaji kesan tahap biasan proses pelapisan Ta dwi-lapisan, kadar aliran nitrogen, tahap biasan proses pelapisan kuprum dan kakisan semula pada lapisan Ta atau TaN pada sifat penuaan rintangan lapisan logam nipis ini. Faktor yang bersignifikan tinggi didapati pada pengkakisan semula lapisan TaN pada logam Ta/TaN dwi-lapisan. Analisis mikrostruktur berkaedah XRD digunakan sebagai rujukan keputusan analisis Rs bagi memahami mekanisme kesan dan ciri-ciri penuaan. Seterusnya, parameter process dari sel-sel eksperimen yang terpilih dan dari sel kontrol telah digunakan dalam penilaian kesan waktu kepada kestabilan Rs di dalam tempoh menunggu antara process pelapisan logam Ta/TaN dwi-lapisan/kuprum dan proses elektrolisis kuprum. Keputusan menunjukkan tiada perbezaan yang ketara walaupun pada 40 jam waktu menunggu. Process terpilih yang merangkumi pengkakisan semula lapisan TaN menunjukkan kestabilan sehingga hampir empat kali ganda berbanding proses standard. Kaedah ini telah menunjukkan nisbah α -Ta dan β -Ta yang lebih tinggi yang dapat menghasilkan lebih banyak butiran Cu(111). Akhirnya, kaedah RSM telah mendapatkan model ramalan bagi meminimumkan perubahan Rs dan ketidakseragamannya semasa penuaan melalui proses pengkakisan semula TaN. Kesannya sekali lagi menunjukkan penguasaannya yang lebih berbanding faktor pemboleh ubah yang lain lalu model ini tidak sesuai untuk ramalan perubahan Rs. Ramalan model bagaimanapun berjaya dijana untuk faktor ketidakseragaman Rs pada 48 jam tempoh penuaan.

ACKNOWLEDGEMENTS

In the Name of Allah, the Most Gracious, the Most Merciful

In the first place, I would like to thank and praise Allah the Almighty, my Creator, my Sustainer, for everything I received since the beginning of my life and granted my prayer to complete the highest level of studies. I would like to extend my appreciation to the Universiti Teknikal Malaysia Melaka (UTeM) for providing the research platform. My sincere appreciation to Silterra Malaysia Sdn Bhd for accommodating this research through its facilities and resources. The support from the management team has been outstanding. Thank you also to the Malaysian Ministry of Higher Education (MOHE) for the financial assistance and the My Brain 15 program offering. Another key assistance which was provided in the baselining phase of this work was through a research grant from Collaborative Research in Engineering, Science and Technology (CREST).

My utmost appreciation goes to my main supervisor, Associate Prof. Dr. Mohd Nizam Abdul Rahman, of Fakulti Kerjuruteraan Pembuatan, Universiti Teknikal Malaysia Melaka (UTeM) for all his support, advice and inspiration. His constant patience for guiding and providing priceless insights during the long 8 years will forever be remembered. My Industrial Advisor, Dr Mohd Azizi Chik, whose never-ending drive and barrier breaking efforts have greatly assist our morale and levelled up my spirits. Very resourceful colleague, Mr. Badrul Hisyam Mahmud who carried out actual processing of the experiments relentlessly. The team from Thin Film Metal department Mr. Adrian, Mr. Zainizan, Ms. Zarifah, Ms. Siti Fatimah and others who have given me precious cooperation in technical research execution and tips.

Last but most importantly, from the bottom of my heart a gratitude to my beloved wife, Puan Rashidah Binti Rahmat, who have been the pillar of strength in all my endeavors, for her encouragements and even technical assistance in my thesis writing. My eternal love also to my other beloved wife Adelina who always support this endeavour tirelessly. All my children, Farhana, Farhan Akmal, Farina Nadia, Aiman Akmal and Irdina Wardah for their patience and understanding of this time sharing challenges. I would also like to thank my beloved parents for their endless support, love and without whom I will not born. Finally, thank you to all the individual(s) who had provided me the assistance, support and inspiration to embark on my study.

TABLE OF CONTENTS

	PAGE
DECLARATION	
APPROVAL	
DEDICATION	
ABSTRACT	ii
TABLE OF CONTENTS	v
LIST OF TABLES	ix
LIST OF FIGURES	xiii
LIST OF SYMBOLS AND ABBREVIATIONS	xxiii
LIST OF APPENDICES	xxvii
LIST OF PUBLICATIONS	xxix
CHAPTER 1 INTRODUCTION	1
1.1 Background	1
1.2 Introduction	1
1.3 Impact of problem	4
1.3.1 Industry approach on the problem	5
1.4 Problem statement	6
1.5 Research objective	6
1.6 Scope of research	7
1.7 Contribution of research	8
1.7.1 Manufacturing quantifiable benefit	9
1.7.2 Unquantifiable benefits on manufacturing	10
1.7.3 Research contribution to the body of knowledge	11
1.8 Thesis Outline	12
CHAPTER 2 LITERATURE REVIEW	14

2.1	Overview of the semiconductor wafer processing	15
2.2	Thin films interconnect in IC manufacturing	20
2.3	Metal thin film	23
2.3.1	Interconnect Materials	24
2.4	Thin-film deposition methods	25
2.4.1	Magnetron sputtering	26
2.5	Cu barrier seed deposition process	34
2.5.1	PVD chamber	37
2.5.2	Supporting process and subsystem	45
2.6	Electroplating process	46
2.7	Cu interconnect film ageing properties	51
2.7.1	Mechanism of Cu interconnect film ageing	51
2.7.2	Properties of Cu interconnect film ageing	57
2.7.3	Desirable ageing property in a Cu interconnect film	59
2.8	Key process parameters	61
2.8.1	Summary of process parameter	64
2.9	Summary of characterization methods	68
2.9.1	Crystal Orientation	70
2.9.2	Sheet Resistance	72
2.9.3	Electron microscope	73
2.9.4	X-Ray diffraction	73
2.9.5	Secondary Ion Mass Spectroscopy	74
2.10	Statistical modelling technique	76
2.10.1	Design of experiment	78
2.10.2	Statistical software	84
CHAPTER 3 METHODOLOGY		87
3.1	Experiment Equipment and Materials	89

3.1.1	Hardware and Parameters	90
3.1.2	Substrate specification	98
3.2	Characterization Method	100
3.2.1	Sheet resistance measurement	101
3.2.2	Transmission Electron Microscope	104
3.2.3	X-Ray Diffraction	108
3.2.4	Secondary Ion Mass Spectroscopy	111
3.3	Experiment Methods	114
3.3.1	Baseline Study	114
3.3.2	Statistical Experiments	117
3.3.3	Validation	124
CHAPTER 4	RESULTS AND DISCUSSION	126
4.1	Results for baseline study	127
4.1.1	Baseline of sheet resistance	127
4.1.2	Microstructure baseline	132
4.1.3	Impact of bi-layer film to Cu barrier seed and electroplated Cu films ageing	136
4.1.4	Impact of trace impurity to bi-layer film	139
4.1.5	Summary of ageing characteristics of baseline CuBS and ECP films	141
4.2	Screening Design of Experiment	142
4.2.1	Fit Model	143
4.2.2	ANOVA analysis for change in mean sheet resistance for Cu Barrier Seed during ageing	146
4.2.3	ANOVA analysis for change in mean sheet resistance for ECP during ageing	147
4.2.4	ANOVA analysis for change in sheet resistance non-uniformity for Cu Barrier Seed and Cu ECP during ageing	153
4.3	Impact of Queue Time after Cu barrier seed	158

4.3.1	Queue time impact to microstructure	163
4.3.2	Grain size characteristics	168
4.3.3	Screening and queue time experiment summary	169
4.4	Optimization and Modelling	170
4.4.1	Rs Mean RSM analysis	173
4.4.2	Rs non-uniformity characteristics derived from RSM analysis	177
4.4.3	Summary of modeling experiment	182
4.5	Model Validation	182
CHAPTER 5	CONCLUSION AND RECOMMENDATIONS	186
5.1	Conclusion	186
5.2	Contributions	189
5.3	Future Work	191
REFERENCES		192
APPENDICES		210



LIST OF TABLES

TABLE	TITLE	PAGE
Table 2.1	Thin film deposition techniques by classification in semiconductor fabrication	26
Table 2.2:	Correlation summary from key studies on Cu ageing characteristics	59
Table 2.3	Effect characteristics of some key deposition parameters on sheet resistance. Re-sputter time which is called etch time influences highly on thickness uniformity (Jacquemin et al., 2005).	61
Table 2.4	Key related studies on the influence of process parameters to sheet resistance and microstructure of the Cu Seed and bi-layer.	65
Table 2.5	Sample of characterization methods used in studying effects of ageing and films properties changes	69
Table 2.6	Summary of experiment designs used in similar studies	79
Table 2.7	Applied statistical DOE and their suitability for this research	81
Table 3.1	Key process parameters used in this study for Cu barrier seed (left) and Cu electroplating (right). Key parameters are highlighted in schematics figures 3.5, 3.7 and 3.9.	91
Table 3.2	Wafer substrate properties used in this research	99

Table 3.3	Measurements and Metrology Tools used	100
Table 3.4	49-Site Contour Map	103
Table 3.5	TEM used in the determination of thickness variation due to substrate bias power and N ₂ levels during TaN/Ta bi-layer and Cu seed deposition	108
Table 3.6	Model and specifications of XRD tool used in this study	109
Table 3.7	Experiment matrix used in baseline study.	115
Table 3.8	Thickness used for each layer in the baseline experiment.	116
Table 3.9	Partial factorial screening experiment	119
Table 3.10	Description of each input parameter in screening experiment and their range	119
Table 3.11	Delay and ageing evaluation matrix used in queue time impact study	121
Table 3.12	Experimental parameters and values used as input and output parameters in RSM modelling experiment	122
Table 3.13	Experiment parameters used compares to an experiment by peer researcher (Tsao et al., 2013)	125
Table 4.1	Derivation of sheet resistance average change data between ageing phase in CuBS Film	129
Table 4.2	Sheet resistance change between ageing phases in ECP Film	131
Table 4.3	Ratio Cu (111) and Ta (110) baseline characteristics before and after 48 hours of ageing.	134

Table 4.4 Cu (111) and Cu(200) detection intensity before and after 48 hours ECP film ageing in baseline sample.	136
Table 4.5 Comparison between standard CuBS and non bi-layer samples showing big variation in Rs ageing characteristics.	137
Table 4.6 Comparison between baseline ECP (Sample C) and non bi-layer samples (Sample D) showing big variation in Rs ageing characteristics.	139
Table 4.7 Percent delta of mean sheet resistance for CuBS and Cu ECP layers from screening experiment	143
Table 4.8 Input impact factor and levels to achieve minimum change in Rs mean	148
Table 4.9 Rs non-uniformity delta between time zero and 48 hours from screening experiment	154
Table 4.10 Summary of impact factor and levels to achieve minimum change in Rs uniformity	157
Table 4.11 Delay and ageing matrix used for queue time impact study	164
Table 4.12 Comparison of XRD peak magnitude between splits after ECP layer 48 hours of ageing	164
Table 4.13 Comparison of peak magnitude between bi-layer samples	167
Table 4.14 Significance of input parameters from fractional factorial screening experiment	170
Table 4.15 RSM Central Cubic Design experiment results 0176486797	172

Table 4.16 Comparison on experiment parameters used in this study and by peer
researcher 175

Table 4.17 Validation trials for percentage Rs non uniformity 183



LIST OF FIGURES

FIGURE	TITLE	PAGE
Figure 1.1	Queue time restriction between CuBS and ECP processes.	3
Figure 1.2	The two components in the Cu interconnect films which are the Cu Electroplating that is deposited on the Cu barrier seed films.	7
Figure 1.3	Wafer quantity with respect to queue time from January to September 2017 (Silterra, 2017)	10
Figure 2.1	Overview of a generic Cu product process flow (Silterra, 2004)	16
Figure 2.2	Schematic of isolation structures layout (Silterra, 2001)	16
Figure 2.3	Schematics of unit CMOS after post gate oxide process. (Silterra, 2001)	17
Figure 2.4	Schematics of post poly silicon, gate spacer and silicide structures. (Silterra, 2001)	18
Figure 2.5	Formation of contact holes through dielectric layers which is aligned to transistor contacts. (Silterra, 2001)	18
Figure 2.6	Interconnect layers from 3 distinct processes to form W filled contact, Cu via, and trench structures. (Silterra, 2001)	19
Figure 2.7	Dual damascene process sequence. (Silterra, 2004)	20

Figure 2.8 Overview of major new techniques in mass manufacturing to support fabrication of high density and high performance interconnect design (Brain, 2016).	22
Figure 2.9 Schematic of magnetron sputtering. B is magnetic flux, E is the direction of Ar ⁺ bombardment. (Brauer, 2014)	29
Figure 2.10 Metal Oxide hysteresis curve with corresponding target and substrate conditions (Adachi et al. 2012)	30
Figure 2.11 Preferential deposition at the trench top due to wider sputter atoms angular distribution (Fulmer et al., 2004)	32
Figure 2.12 Schematic representation of the plasma confinement observed in conventional and unbalanced magnetrons (Kelly and Arnell, 2000).	33
Figure 2.13 Re-sputtering reduce via bottom barrier thickness and improve step coverage. (Y. Wang et al., 2008)	34
Figure 2.14 Interfacial failure between bottom trench and top via due to interfacial Cu oxidation necessitates preprocess chambers (Silterra, 2017)	35
Figure 2.15 Areas defined as sidewall and bottom coverage in a plug or via structure (Fulmer et.al. 2004)	36
Figure 2.16 Layer diagram of prepared samples in Cu barrier seed process which consist of Cu Seed/TaN/Ta bi-layer /SiO ₂ /Si substrate	37
Figure 2.17 A schematic diagram of DC plasma sputtering (Chiang et al., 2001).	38
Figure 2.18 Location of magnetron and the various arrangement of magnetic pieces in a magnetron assembly in a sputtering chamber. (Ding et al., 2014)	39

Figure 2.19 Cryogenic pump system consists of cold head, compressor and pressure reader (Ideal Vacuum Products, 2020)	40
Figure 2.20 Dual damascene structure with Cu and TaN/Ta bi-layer deposition layers (Teh and Singham, 2008)	41
Figure 2.21 TaN/Ta bi-layer deposition chamber known as Encore™ Ta deposition chamber (Ding et al., 2014)	42
Figure 2.22 Cu deposition chamber known as SIP Cu deposition chamber (Chiang et al., 2001)	44
Figure 2.23 Material Research Corporation MRC943 batch sputtering system (CPA Sputtering System, n.d.)	46
Figure 2.24 Applied Materials Endura P5500 cluster tool (Applied Materials, 2020)	46
Figure 2.25 TEM picture of High Aspect Ratio via with clear overhang of Cu seed layer (Besling et al., 2004)	47
Figure 2.26 Cu interconnect structure of vias and trenches with insulator removed. (Kim, 2002)	48
Figure 2.27 Dual Damascene process of creating interconnect layer (Olawumi, 2015)	48
Figure 2.28 Steps of Cu Bulk Layer Electroplating Process.	49
Figure 2.29 Unit cell of α -Ta and β -Ta atomic arrangement (Tsao et al., 2013)	52

Figure 2.30 Normalized sheet resistance as a function of time, for three blanket layers of thickness = 0.5, 0.75, and 1.0um from top to bottom respectively (Brongersma et al., 1999).	54
Figure 2.31 sheet resistance of barrier seed films with different barrier processes (Chen <i>et als.</i> , 2002)	55
Figure 2.32 Correlation of the intensity ratio for the (111)/(200) in the copper layer between Cu ECP and seed layers (Hara et al., 2002)	56
Figure 2.33 Evolution of crystallite size indicating slower growth of 111 Cu (Pantleon and Somers, 2010)	60
Figure 2.34 Relationship between re-sputter, nitrogen flow TaN deposition, and resultant sheet resistance (Y. Wang et al., 2008).	64
Figure 2.36 Grain size dependency on Cu layer thickness, underlayer metal and process condition.	71
Figure 2.37 A pulsed primary ion gun is focused on and scanned over the sample surface (left). Secondary ions are extracted into the parallel imaging spectrometer (right). Image by IONTOF GmbH, Munster, Germany.	75
Figure 2.38 SEMATECH qualification plan for process and equipment characterization and improvement (Czitrom and Horrell, 1997)	77
Figure 3.1 Research phases in this study	88
Figure 3.2 Process flow block diagram and cross section schematics for each process steps related to this study	89

Figure 3.3 Schematic of deposition equipment with process sequence number. The flow chart displays the path for Cu barrier seed deposition process stations.	90
Figure 3.4 Image of a degas chamber used in the experimental setup to remove moisture from a wafer	92
Figure 3.5 Degas schematics indicating heat source (halogen bulb) and wafer location during process	92
Figure 3.6 Encore [®] Ta(N) chamber used in the experimental setup to deposit TaN/Ta barrier layer	93
Figure 3.7 Schematic of Encore [®] Ta deposition chamber linking its key process components to parameters used in the study highlighted in black.	94
Figure 3.8 Encore [®] Cu chamber used in the experimental setup to deposit Cu seed film	95
Figure 3.9 Schematic of Encore [®] Cu deposition chamber linking its key process components to parameters used in the study highlighted in black.	95
Figure 3.10 Process flow of a wafer during electroplating processing steps (Ngai, 2004)	96
Figure 3.11 Overview of Copper Electroplating Cell (Applied Materials, 2002)	97
Figure 3.12 4 point probe measurement concept	101
Figure 3.13 Sheet resistance measurement tool KLA-Tencor RS-100	102

Figure 3.14 Gauge RnR study for Rs100 sheet resistance measurement tool (Silterra, 2017)	104
Figure 3.15 Carl Zeiss AG - LIBRA 200 FE	107
Figure 3.16 Bruker D-8 Advance tool used in this research	109
Figure 3.17 XRD sample preparation. Sample cutting step prior to analysis (right). Multi sample holder queuing for analysis (left).	111
Figure 3.18 PHI Adept 1010 SIMS analyzer (Ulvac-PHI Inc, 2021).	112
Figure 3.19 Layer schematics and SIMS analysis sampling flow.	113
Figure 3.20 Baseline study with stacks of sample A (left) and sample B (right). Sample A as is standard process while B without bi-layer TaN/Ta	117
Figure 3.21 Stacks that includes standard Cu plating film sample C (left) and without the bi-layer film in sample D (right).	117
Figure 3.22 Plot of parameters used in the CCD RSM experiment	123
Figure 4.1 Plot of sheet resistance mean reduction over ageing time from 12 to 300 hours for CuBS film	127
Figure 4.2 Average percent change of sheet resistance profile over ageing period for Cu barrier seed film.	128
Figure 4.3 Plot of sheet resistance average measured during ageing from 12 to 300 hours of ageing times after ECP process	129
Figure 4.4 A 3 rd degree polynomial shows high goodness of fit for the first 36 hours.	130

Figure 4.5 Percentage Rs reduction based on accumulative and hourly change for Cu ECP film	130
Figure 4.6 XRD profile for crystal orientations of baseline process Cu barrier seed (CuBS) film at t<12 hours and 48 hours ageing	133
Figure 4.7 XRD profile for crystal orientations of Cu ECP film at 0 and 48 hours ageing time	135
Figure 4.8 Drastic difference in Rs change during ageing in CuBS samples	137
Figure 4.9 Comparison between standard ECP and sample without bi-layer indicating an earlier ageing influence on Rs for the later sample. Phase identifier lines are based on a standard ECP sample.	138
Figure 4.11 Oxygen atomic density profiles comparison between standard and barrier-less film stacks.at different queue time between CuBS and ECP processes	140
Figure 4.12 Model Fit and ANOVA analysis for percent delta in mean Rs for Cu barrier seed (left) and Cu ECP(right) after 48hrs ageing	145
Figure 4.13 Effect test table from ANOVA analysis for Cu barrier seed film Rs ageing after 48 hours	146
Figure 4.14 Effect test table from ANOVA analysis for ECP film Rs ageing after 48 hours	147
Figure 4.15 Scaled estimates chart for Cu barrier seed mean Rs after ageing at 48 hours	148
Figure 4.16 Scaled estimates chart for Cu ECP mean Rs after ageing at 48 hours	149